

Origins of the Viscosity Peak in Wormlike Micellar Solutions. 1. Mixed Catanionic Surfactants. A Cryo-Transmission Electron Microscopy Study

Lior Ziserman,[†] Ludmila Abezgauz,[†] Ory Ramon,[†] Srinivasa R. Raghavan,[§] and Dganit Danino^{*†‡}

[†]Department of Biotechnology and Food Engineering and [‡]Russell Berrie Nanotechnology Institute, Technion-Israel Institute of Technology, Haifa, Israel 32000, and [§]Department of Chemical and Biomolecular Engineering, University of Maryland, College Park, Maryland 20742-2111

Received April 4, 2009. Revised Manuscript Received May 23, 2009

The rheology of wormlike micelles (“worms”) formed by surfactants in water often follows nonmonotonic trends as functions of composition. For example, a study by Raghavan et al. (*Langmuir* **2002**, *18*, 3797) on mixtures of the anionic surfactant sodium oleate (NaOA) and the cationic surfactant octyl trimethylammonium bromide (OTAB) reported a pronounced peak in the zero-shear viscosity η_0 as a function of NaOA/OTAB ratio at a constant surfactant concentration (3 wt %). In this work, we study the origins of rheological changes in the NaOA/OTAB system and the relations between the composition and structural characteristics using cryo-transmission electron microscopy (cryo-TEM). When either surfactant is in large excess, the dominating morphology is that of spherical micelles. As oppositely charged surfactant is added to the mixture, the spheres grow into linear worms and these continue to elongate as the viscosity peak (which occurs at a 70/30 NaOA/OTAB ratio) is approached from either end. At the viscosity peak, the sample shows numerous long worms as well as a small number of branched worms. Taken together, NaOA/OTAB rheology can be primarily understood on the basis of micellar growth, which is explained primarily by packing arguments. While the size of the hydrophobic micellar core continuously decreases as the short amphiphile OTAB is added at the expense of NaOA, screening of charges goes through a maximum, which contributes to the asymmetry of the viscosity curve. With regard to micellar branching, there is no significant difference in the density of branched worms on either side of the viscosity peak. Therefore, it appears that in contrast to the behavior of some surfactant/salt systems, branching does not have a significant influence on the rheology of this mixed catanionic surfactant system. Instead, our data clearly indicate that the origin of the viscosity peak is linked with micellar growth and micellar shortening.

1. Introduction

Wormlike micelles (“worms”) make up a fascinating class of self-assembled structures formed by surfactants in water. These long, flexible cylindrical chains, with contour lengths as long as several micrometers, can entangle into transient networks, leading to the appearance of viscoelastic properties in the fluid.^{1–3} Accordingly, worms have attracted much attention from industry as rheology modifiers in commercial products.⁴ They have also been of great interest to soft matter physicists because of their similarities to high-molecular weight polymers. Unlike polymers, whose chain length is fixed by covalent bonds, worms are considered to be “living” polymers because they can break and re-form, and their length is thus controlled by thermodynamics (composition and temperature).^{2,3}

There are several ways to create worms. One is to combine a long-tailed ionic surfactant [e.g., cetylpyridinium chloride

(CPyCl)] with salt. Both inorganic salts (like sodium chloride) and organic salts [like sodium salicylate (NaSal)] can be used.^{5–8} Alternatively, it is possible to combine two surfactants, either one ionic and the other nonionic,⁹ or surfactants of opposite charge.¹⁰ An example of the latter is the study by Raghavan et al.¹¹ on mixtures of sodium oleate (NaOA), a C₁₈-tailed anionic surfactant, and octyl trimethylammonium bromide (OTAB), a C₈-tailed cationic surfactant. The principle behind the above approaches is the same: “binding” of salt counterions or the second surfactant to the micelles of the former ionic surfactant, reducing the net charge and thereby the electrostatic repulsions between headgroups. In turn, the net surfactant geometry becomes conductive to growth from spheres to cylinders/worms.³

An intriguing feature of wormlike micellar systems is the existence of nonmonotonic trends in rheological properties. For example, consider the zero-shear viscosity η_0 , i.e., the viscosity in the limit of low shear rates. A plot of η_0 versus salt concentration in surfactant/hydrotrope systems like CPyCl/NaSal^{1,12} and C₁₆TAB/NaSal¹³ generally shows a first pronounced peak, followed by a trough, and then a second moderate peak. A peak

*To whom correspondence should be addressed. E-mail: dganitd@tx.technion.ac.il.

- (1) Rehage, H.; Hoffmann, H. *J. Phys. Chem.* **1988**, *92*, 4712–4719.
- (2) Cates, M. E. *Macromolecules* **1987**, *20*, 2289–2296.
- (3) Candau, S. J.; Oda, R. *Colloids Surf., A* **2001**, *183*, 5–14.
- (4) Magid, L. J. *J. Phys. Chem. B* **1998**, *102*, 4064–4074.
- (5) Croce, V.; Cosgrove, T.; Maitland, G.; Hughes, T.; Karlsson, G. *Langmuir* **2003**, *19*, 8536–8541.
- (6) Rehage, H.; Hoffmann, H. *Mol. Phys.* **1991**, *93*–973.
- (7) Oelschlaeger, C.; Waton, G.; Candau, S. J. *Langmuir* **2003**, *19*, 10495–10500.
- (8) Oelschlaeger, C.; Schopferer, A.; Scheffold, F.; Willenbacher, N. *Langmuir* **2009**, *25*, 716–723.

(9) Croce, V.; Cosgrove, T.; Dreiss, C. A.; Maitland, G.; Hughes, T.; Karlsson, G. *Langmuir* **2004**, *20*, 7984–7990.

(10) Koehler, R. D.; Raghavan, S. R.; Kaler, E. W. *J. Phys. Chem. B* **2000**, *104*, 11035–11044.

(11) Raghavan, S. R.; Fritz, G.; Kaler, E. W. *Langmuir* **2002**, *18*, 3797–3803.

(12) Hoffmann, H. In *Structure and Flow in Surfactant Solutions*; Herb, C. A., Robert, K., Eds.; American Chemical Society: Washington, DC, 1994; Vol. 578.

(13) Hartmann, V.; Cressley, R. *Colloid Polym. Sci.* **1998**, *276*, 169–175.

is also often created when inorganic salts are added to surfactants.^{5,14,15} Both the growth rate and the peak viscosity value strongly depend on molecular characteristics as well as on physicochemical parameters of the system. Although these parameters strongly vary between studies, it is generally found that the changes induced by nonpenetrating additives are more moderate, and the peak viscosity in those systems typically reaches 10–100 Pa·s, compared with a zero-shear viscosity value of >1000 Pa·s observed with the penetrating, organic aromatic salts.

A single pronounced peak has also been reported in numerous charged^{16,17} and uncharged systems¹⁸ and in mixed surfactant systems.^{10,11,19} In the NaOA/OTAB system, for example, a peak in the plot of η_0 versus composition is obtained at a NaOA/OTAB ratio of 70/30 when the total surfactant concentration is fixed at 3 wt%, with a peak η_0 that is 1 million-fold higher than the viscosity of pure NaOA or OTAB solutions.¹¹ A detailed review of these studies was recently published by Dreiss.²⁰

Why does the viscosity of worms go through a peak as a function of surfactant ratio or salt content? Two hypotheses dominate the literature. The first is that the worms grow while staying linear up to the peak, whereas beyond the peak, linear worms transform into branched (also called connected) networks.^{5,6,11,19,21–25} Theoretical studies have predicted that branching of worms should lower the viscosity, and so there is a foundation for this hypothesis.²⁶ The second hypothesis is that the worms grow up to the peak and shrink beyond the peak.^{4,27,28} Currently, which of the models described above is right is an open question. One reason why this problem is complicated is because it is not easy to distinguish between linear and branched worms using conventional techniques such as rheology, light scattering, or neutron scattering.^{5,29,30} The most reliable way to confirm branches in worms is the technique of cryo-transmission electron microscopy (cryo-TEM), which allows unambiguous direct visualization of the structures present in a micellar sample.^{5,29–32}

So far, to the best of our knowledge, only a few studies have applied cryo-TEM to investigate the viscosity peak in a wormlike micellar system.^{5,30,33,34} In particular, Croce et al.⁵ studied worms formed by the cationic surfactant, erucyl bis(hydroxyethyl)methylammonium chloride (EHAC), and potassium chloride (KCl).

- (14) Cappaer, E.; Cressely, R. *Colloid Polym. Sci.* **1998**, *276*, 1050–1056.
- (15) Candau, S. J.; Khatory, A.; Lequeux, F.; Kern, F. *J. Phys. IV* **1993**, *3*, 197–209.
- (16) Tobita, K.; Sakai, H.; Kondo, Y.; Yoshino, N.; Iwashashi, M.; Momozawa, N.; Abe, M. *Langmuir* **1997**, *13*, 5054.
- (17) Danino, D.; Weih, D.; Zana, R.; Orädd, G.; Lindblom, G.; Abe, M.; Talmon, Y. *J. Colloid Interface Sci.* **2003**, *259*, 382–390.
- (18) Acharya, D. P.; Kunieda, H. *J. Phys. Chem. B* **2003**, *107*, 10168–10175.
- (19) Acharya, D. P.; Hattori, K.; Sakai, T.; Kunieda, H. *Langmuir* **2003**, *19*, 9173–9178.
- (20) Dreiss, C. A. *Soft Matter* **2007**, *3*, 956–970.
- (21) Schubert, B. A.; Kaler, E. W.; Wagner, N. J. *Langmuir* **2003**, *19*, 4079–4089.
- (22) Ali, A. A.; Makhloufi, R. *Phys. Rev. E* **1997**, *56*, 4474–4478.
- (23) Hartmann, V.; Cressely, R. *Rheol. Acta* **1998**, *37*, 115–121.
- (24) Khatory, A.; Kern, F.; Lequeux, F.; Appell, J.; Porte, G.; Morie, N.; Ott, A.; Urbach, W. *Langmuir* **1993**, *9*, 933–939.
- (25) Croce, V.; Cosgrove, T.; Dreiss, C. A.; King, S.; Maitland, G.; Hughes, T. *Langmuir* **2005**, *21*, 6762–6768.
- (26) Lequeux, F. *Europhys. Lett.* **1992**, *19*, 675–681.
- (27) Imae, T.; Kohsaka, T. *J. Phys. Chem.* **1992**, *96*, 10030–10035.
- (28) Cappaer, E.; Cressely, R. *Rheol. Acta* **2000**, *39*, 346–353.
- (29) Ambrosone, L.; Angelico, R.; Ceglie, A.; Olsson, U.; Palazzo, G. *Langmuir* **2001**, *17*, 6822–6830.
- (30) Lin, Z. *Langmuir* **1996**, *12*, 1729–1737.
- (31) Danino, D.; Bernheim-Groswasser, A.; Talmon, Y. *Colloids Surf., A* **2001**, *183*, 113–122.
- (32) Danino, D.; Talmon, Y.; Levy, H.; Beinert, G.; Zana, R. *Science* **1995**, *269*, 1420–1421.
- (33) Clausen, T. M.; Vinson, P. K.; Minter, J. R.; Davis, H. T.; Talmon, Y.; Miller, W. G. *J. Phys. Chem.* **1992**, *96*, 474–484.
- (34) Lin, Z.; Cai, J. J.; Scriven, L. E.; Davis, H. T. *J. Phys. Chem.* **1994**, *98*, 5984–5993.

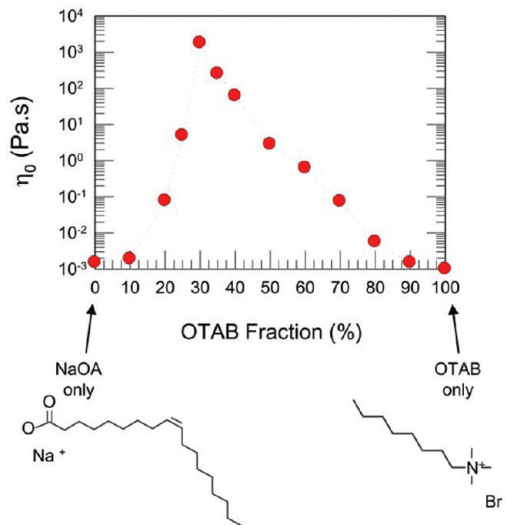


Figure 1. Zero-shear viscosity η_0 of NaOA/OTAB mixtures as a function of OTAB weight fraction in the mixture. The total surfactant concentration is 3 wt%. The structures of the individual surfactants, NaOA and OTAB, are also shown. This figure was reproduced from ref 11. Copyright 2002 American Chemical Society.

EHAC/KCl worms at 1.5% EHAC showed a single peak in η_0 when plotted as a function of KCl concentration. Cryo-TEM conducted on selected samples along this viscosity curve revealed mainly linear worms to the left of the peak, and mostly branched worms to the right of the peak. These data support the idea that the peak in η_0 signifies a transition from linear to branched worms and that the drop in viscosity occurs when branched worms emerge as the dominant structure in the sample.

In this study, we apply cryo-TEM to the mixed NaOA/OTAB system, which was thoroughly studied by Raghavan et al.¹¹ using rheology and neutron scattering. From the various rheological parameters determined in that study, we selected specifically the zero-shear viscosity, whose trends are the hallmark of changes in the nanostructure of the micelles, with the aim of clarifying the origin of the viscosity peak and the viscosity drop reported as a function of surfactant composition. Specifically, we fix the total surfactant content at 3 wt% and vary the NaOA/OTAB ratio (the corresponding data for η_0 are replotted in Figure 1). We seek to correlate sample microstructure, as determined by cryo-TEM, with the zero-shear viscosity. On the basis of our results, we conclude that the rheology in this system is primarily impacted by changes in micellar length rather than by transitions from linear to branched micelles.

2. Experimental Section

Materials and Sample Preparation. The compounds *n*-hexyl trimethylammonium bromide [$C_6H_{13}N(CH_3)_3Br$, C₆TAB], *n*-octyl trimethylammonium bromide [$C_8H_{17}N(CH_3)_3Br$, OTAB], *n*-dodecyl trimethylammonium bromide [$C_{12}H_{25}N(CH_3)_3Br$, C₁₂TAB], and sodium oleate (*cis*-9-octadecanoate, $C_9H_{18}=C_8H_{15}COONa$, NaOA) were obtained from TCI America (>99% pure) and used as received. C₆TAB does not form micelles and has no CMC. OTAB is the surfactant with the shortest alkyl chain in the TAB⁺ family. Distilled and deionized water was used in preparing the mixed surfactant solutions. First, 3 wt% solutions of each surfactant were made. After equilibration for 24 h at room temperature, mixtures of the two solutions (OTAB and NaOA) at various ratios were prepared. The samples we studied were completely clear and transparent, with a pH of

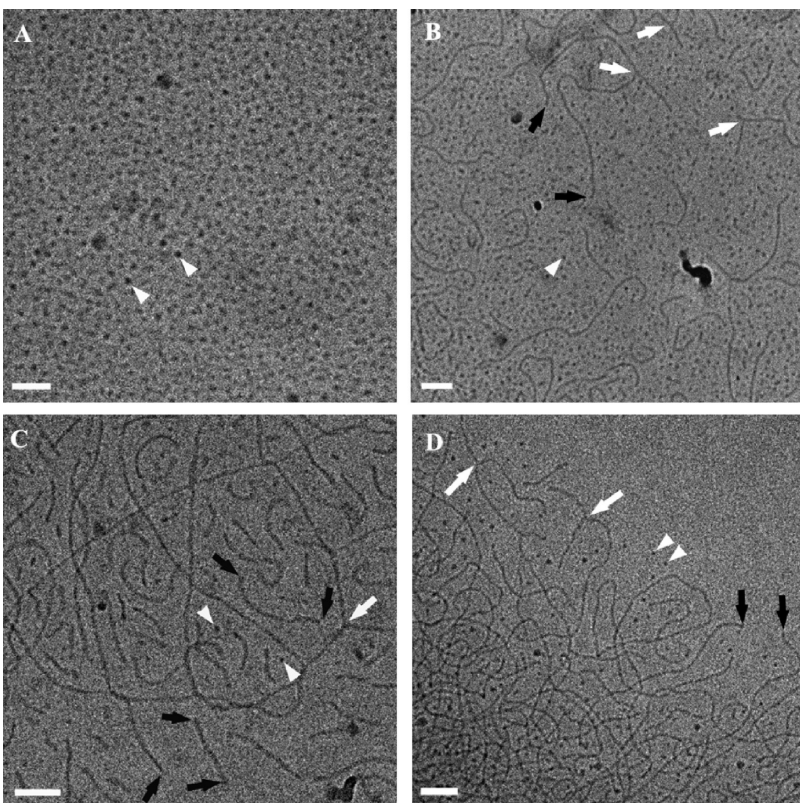


Figure 2. Cryo-TEM images of NaOA/OTAB structures left to the viscosity peak. OTAB concentrations equal 0 (A), 10 (B), 15 (C), and 20 wt% (D). The images show the gradual decrease in the number of spherical micelles (denoted with white arrowheads) coupled with the formation of worm micelles with increasing length, as more OTAB is added to the mixture. Also evident is the decreasing number of end caps as the OTAB concentration increases (black arrows). Micellar growth is further accompanied by the formation of junction points, as denoted with the white arrows. While all junctions are of the three-fold variety, they display diverse local connection angles (compare for example the angles in panels C and D). Bars are 50 nm.

~11.5 in OTAB-free samples, and decreasing down to a pH of ~8.3 at 10/90 NaOA/OTAB samples. Similar procedures were used to prepare C₆TAB/NaOA mixtures at ratios near the viscosity peak and C₁₂TAB/NaOA mixtures at a cationic surfactant excess.

Cryo-TEM. Specimens were prepared in a controlled environment vitrification system (CEVS) at 25 °C and 100% relative humidity. A drop of solution was placed on a TEM grid covered with a perforated carbon film and blotted with a filter paper to form a thin solution film on the grid. The exact amount of blotting and its mode of application were adjusted so as to obtain films ranging between 100 and 250 nm in thickness. The blotted samples were allowed to stand in the CEVS for 10–30 s to relax from shearing effects caused by the blotting. The relaxed samples were then plunged into liquid ethane at its freezing temperature (−183 °C) to form vitrified specimens and stored at −196 °C in liquid nitrogen until examination. Specimens were examined in a Philips CM120 transmission electron microscope optimized for cryo-TEM work. The microscope was operated at an accelerating voltage of 120 kV using an Oxford CT3500 cryo-specimen holder that maintained the vitrified specimens below −175 °C. Specimens were examined in the low-dose imaging mode to minimize electron-beam radiation damage. Images were recorded digitally at nominal magnifications up to 175000× on a cooled Gatan Multi-Scan 791 CCD camera, using the DigitalMicrograph software.^{31,35}

3. Results

Rheological data on the NaOA/OTAB system at a total surfactant concentration of 3 wt % are reproduced in Figure 1.

The data show the zero-shear viscosity η_0 of the mixtures versus the OTAB content in the mixture. As noted earlier, η_0 peaks at a 70/30 NaOA/OTAB weight ratio, which corresponds to ~2:1 NaOA/OTAB molar ratio. The peak η_0 is ~1 million-fold higher than the viscosities of pure NaOA and pure OTAB solutions.

We use cryo-TEM to probe the microstructures in the NaOA/OTAB mixtures described above. We start with samples on the NaOA-rich end of Figure 1 (to the left of the viscosity peak). First, consider 3 wt % NaOA alone (i.e., 100/0 NaOA/OTAB). In this sample, spherical micelles ~4 nm in diameter prevail. Several such micelles are marked by white arrowheads in Figure 2A. The existence of only spherical micelles is consistent with the low viscosity of 1.5 mPa·s of this sample. Note that 3 wt % is well above the critical micelle concentration (CMC) of NaOA, which is 0.06 wt %.

Next, we turn to the 90/10 NaOA/OTAB solution, which is again a Newtonian, low-viscosity solution with a viscosity of 3 mPa·s. In this case, cryo-TEM shows spherical micelles coexisting with short, flexible, worms (Figure 2B). The end caps of several worms (black arrows in Figure 2B) can be distinguished, and the end-to-end or contour length \bar{L} of those worms can thus be estimated: \bar{L} ranges from 50 to 300 nm. In addition, a few branch points (junctions), typically 3-fold, are seen in this sample. The presence of junctions is intriguing since spherical micelles and junctions represent limits of high and low curvature, respectively, in micellar solutions.³⁶ However, occasional

(35) Cui, H.; Hodgdon, T. K.; Kaler, E. W.; Abetzgauz, L.; Danino, D.; Lubovsky, M.; Talmon, Y.; Pochan, D. J. *Soft Matter* 2007, 3, 945–955.

(36) May, S.; Bohbot, Y.; BenShaul, A. *J. Phys. Chem. B* 1997, 101, 8648–8657.

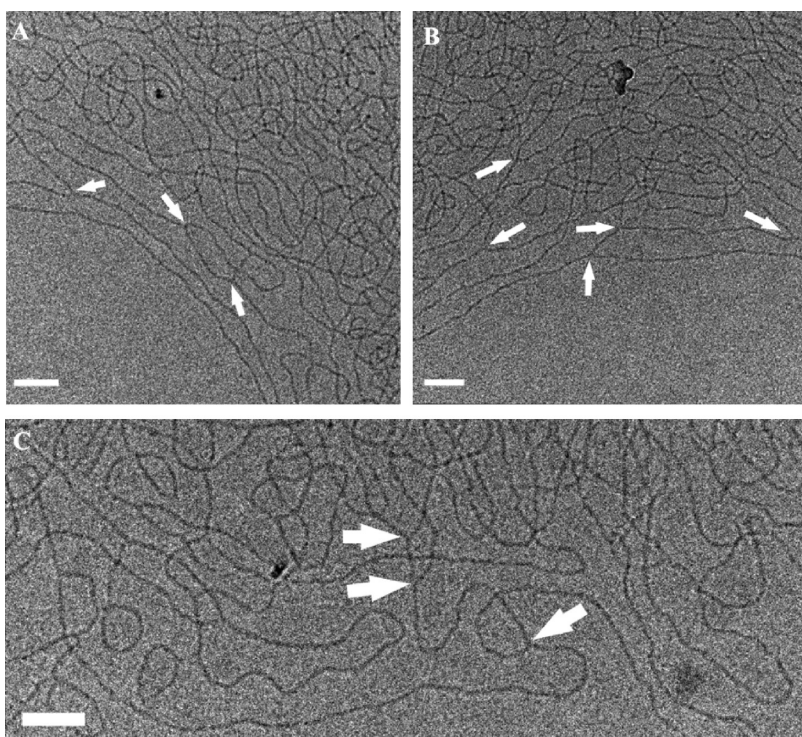


Figure 3. Cryo-TEM images of 70/30 NaOA/OTAB samples, which exhibit the highest zero-shear viscosity. No spherical micelles, short wormlike micelles, or end caps are found at this composition, which implies the micelles are at their longest form. However, 3-fold junctions do form, as denoted with white arrows. Bars are 50 nm.

junctions may arise from local inhomogeneity in the concentration (local demixing), which has been seen in some multicomponent systems.^{37–39}

Between 90/10 and 70/30 NaOA/OTAB ratios, the viscosity increases exponentially (Figure 1), and we therefore followed the sample structure in small composition intervals. Images for the 85/15 and 80/20 samples are given in panels C and D of Figure 2, respectively, and Figure 3 shows several images of the 70/30 sample. While a quantitative analysis of the structural features cannot be made on the basis of the images, the trends we see with a change in composition are clear and can be analyzed. The 85/15 sample, which has a viscosity η_0 of 10 mPa·s, reveals mostly worms with a few remnant spherical micelles (Figure 2C). Some of the worms are short ($\bar{L} \sim 50$ –100 nm), while others are relatively long ($\bar{L} \sim 500$ –1000 nm). Further elongation of the worms is clearly seen in the 80/20 sample (Figure 2D), which has an η_0 of 100 mPa·s, i.e., 10 times higher than that of the 85/15 sample. It is difficult to estimate \bar{L} for these worms, as the micellar ends are rarely seen in the field of view. However, from low-magnification images, we estimate that \bar{L} can range up to several micrometers. In addition to the long worms, the 80/20 sample also shows a few spherical micelles and a few branch points (white arrowheads and arrows in Figure 2D, respectively).

Turning now to the 70/30 sample (viscosity peak; $\eta_0 = 1800$ Pa·s), we find worms in their longest form in this case (Figure 3), and there is extensive overlap and entanglement of the worms. Spherical micelles are totally absent from the images. Micellar end caps are rare, even in low-magnification images, and we therefore estimate \bar{L} to reach tens of micrometers. In addition to long, entangled worms, there are also a few branch points (3-fold

junctions; white arrows) in the images shown in Figure 3. While linear worms dominate in all images recorded at the peak composition, only few branched micelles were detected. Similar results were found for the NaOA/C₆TAB system in the vicinity of the viscosity peak (see the Supporting Information).

All images in Figure 3 show relatively thin vitrified regions; however, they also display the typical thickness gradient of cryo-TEM samples. The center of the film (bottom left region in Figure 3A and bottom part of Figure 3B) is very thin and hence devoid of structures. When one moves toward the thicker edges, individual assemblies and then overlapping structures are observed. Slight alignment of worms is observed in the intermediate region, whereas in the thicker regions, the worms are unaligned and entangled. We emphasize that the structural details described here are indeed characteristic of the sample, and they represent data found in many (tens to hundreds) images collected on multiple samples. For the most part, the worms are relaxed and entangled, indicating that sufficient time has been allotted for the worms to relax following blotting and before vitrification.

We now move on to NaOA/OTAB samples to the right of the viscosity peak. Panels A and B of Figure 4 show images of the 60/40 and 50/50 samples, which have viscosities (η_0) of 60 and 2 Pa·s, respectively (these are much lower compared to the peak η_0 of 1800 Pa·s for the 70/30 sample). Both of these samples contain entangled/overlapped worm micelles. In addition, the images show a few branch points (white arrows), some closed micellar rings (red arrows), and a few micellar end caps (black arrows).

Since the distinction between branched and overlapped micelles is sometimes a subtle one, we pinpoint in panels A and B of Figure 4 a few clear 3-fold branch points (white arrows). With regard to end caps, there are definitely more of them in the 50/50 than in the 60/40 sample (see the black arrows). The 50/50 sample also shows distinct spherical micelles (white arrowheads).

(37) Dan, N.; Shimoni, K.; Pata, V.; Danino, D. *Langmuir* **2006**, *22*, 9860–9865.

(38) Shimoni, K.; Danino, D. *Langmuir* **2009**, *25*, 2736–2742.

(39) Zhang, Y.; Schmidt, J.; Talmon, Y.; Zakin, J. L. *J. Colloid Interface Sci.* **2005**, *286*, 696–709.

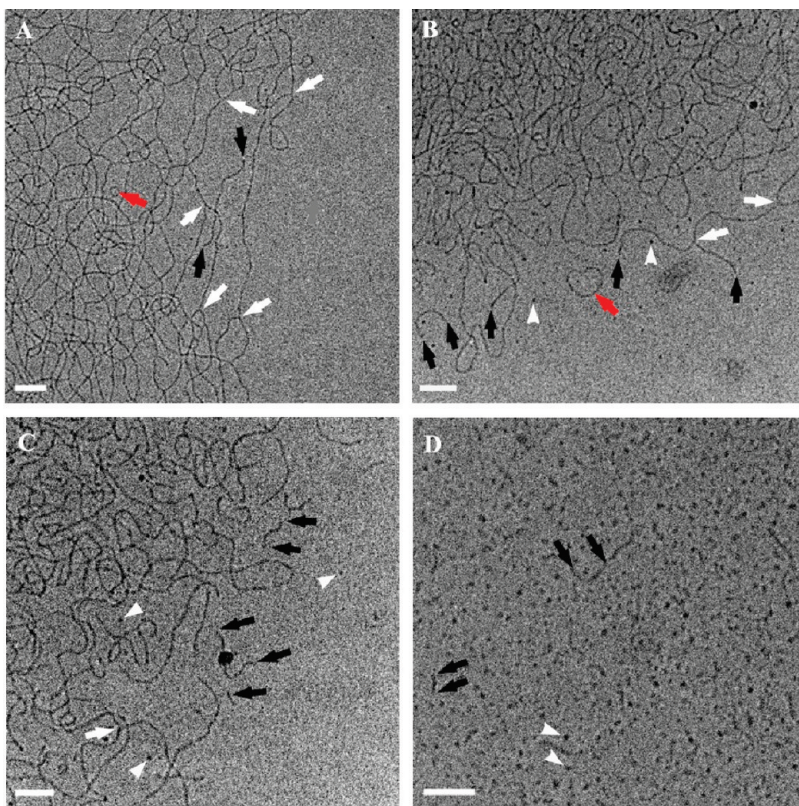


Figure 4. Cryo-TEM images of NaOA/OTAB samples right to the viscosity peak. OTAB concentrations equal to 40 (A), 50 (B), 80 (C), and 90 wt% (D). The images show the gradual decrease in the worm micelle length as more OTAB is added to the mixture. This is accompanied by the formation of an increasing number of end caps (denoted with black arrows) and spherical micelles (white arrowheads), until eventually, almost only spherical micelles exist (D). Like in other regions, 3-fold junction points connecting micellar segments are visible (denoted with white arrows). Some rings are also occasionally found, and a few are marked with red arrows. Bars are 50 nm.

Together, the end caps and spherical micelles in the 50/50 sample suggest an overall lowering of the micellar length \bar{L} compared to that in the 70/30 sample.

Moving further beyond the peak into the OTAB-rich side, we provide images of the 20/80 and 10/90 samples in panels C and D of Figure 4, respectively. The micellar shortening seen in the 50/50 sample further continues in these samples, and the 20/80 sample ($\eta_0 = 5 \text{ mPa}\cdot\text{s}$) shows numerous short worms coexisting with a considerable population of spherical micelles. Finally, the 10/90 sample ($\eta_0 = 1 \text{ mPa}\cdot\text{s}$, i.e., that of water) contains mostly spherical micelles $\sim 4\text{--}5 \text{ nm}$ in diameter and just a few rodlike micelles of length $\bar{L} \sim 20\text{--}50 \text{ nm}$ (end caps denoted with black arrows). Note that the CMC of OTAB is 3.5 wt%, so a pure OTAB sample at 3 wt% does not form micelles. However, micelles do exist in the 10/90 sample, i.e., when a small amount of NaOA is present in the mixture. Such micellization is promoted due to the synergy between the two oppositely charged surfactants.^{10,11,19}

4. Discussion

We used here direct imaging cryo-TEM to correlate the viscosity with the nanostructure of the micelles and to elucidate the origin of the viscosity peak described in Figure 1. In our system, the solution composition was varied by replacing molecules of the long-chain NaOA with the oppositely charged short-chain OTAB while keeping the total surfactant concentration fixed at 3 wt%. It is worth mentioning that this concentration is much higher than the NaOA CMC (0.06 wt%) yet less than the OTAB CMC (3.5 wt%).

Two distinct factors contribute collectively to the micellar behavior we identified: changes in the molecular packing and

changes in the effective composition. The variation in the molecular packing can be understood by examining P , the packing parameter, a powerful dimensionless parameter that relates geometrical characteristics of the molecules with the micellar shape. P is given by the equation $P = v/a_0 l_c$, where v is the chain hydrophobic volume, l_c the chain length, and a_0 the effective area per headgroup the molecules occupy at the micellar interface.⁴⁰ Small P values of $\sim 1/3$ indicate the formation of highly curved assemblies (spherical micelles), while higher P values of $\sim 1/2$ refer to moderately curved structures (cylindrical micelles). Adding the short-chain surfactant OTAB at the expense of NaOA affects both the hydrophobic volume and the area per headgroup that are expressed in the P , but in a different mode. The effective headgroup area passes through a minimum (thus P through a maximum) as the surface charge density varies from that of fully charged anionic micelles to zero at an equimolar ratio (reached at a weight ratio of 55/45) and then increases again as the cationic surfactant is further added and the micelle continuously acquires net positive charge. The hydrophobic volume, on the other hand, is continuously decreasing as OTAB is added at the expense of NaOA. Similarly, the effective surfactant concentration continuously decreases throughout the entire composition window we studied, until in a pure OTAB solution it reaches below the solution CMC.

It is now useful to step back and absorb the cryo-TEM and rheology data in their entirety. If we compare samples on either end of Figure 1 (mostly NaOA, e.g., 90/10, or mostly OTAB,

(40) Israelachvili, J. N.; Mitchell, D. J.; Ninham, B. W. *J. Chem. Soc., Faraday Trans. II* 1976, 72, 1525–1568.

e.g., 10/90) with those mixtures toward the middle of Figure 1, the trends are clear. Starting from pure NaOA and proceeding up to the viscosity peak, we observe a tremendous increase in viscosity, and this is accompanied by micellar growth. The structural pattern is from only spheres (100/0) to spheres with short worms (90/10) to fewer spheres with longer worms (85/15 and 80/20) and finally to only very long slightly branched worms (70/30). Similarly, if we start from the OTAB end and proceed toward the viscosity peak, we again see a consistent pattern of micellar growth. Again, the pattern is from mostly spheres (10/90) to a few spheres with short worms (20/80) to a few spheres with longer/branched worms (50/50 and 60/40). Thus, on both sides of the peak, introducing the oppositely charged surfactant into the mixture causes the micelles to grow and eventually become long wormlike chains.

Let us now analyze this data by considering the factors affecting the assembly to the left and right of the viscosity peak.

Micellar Growth in Excess NaOA. When only NaOA is present in the solution, the electrostatic repulsions between the headgroups are strong, leading to a large effective area per surfactant headgroup. This scenario favors the formation of spherical micelles, which are characterized by a P of $\sim 1/3$.⁴⁰ When the oppositely charged surfactant OTAB is added and intercalates into the micelles, the net surface charge on the micelles is reduced, and thereby, the effective area per headgroup is decreased. As a result, a transition in micellar geometry from spheres to cylinders (rods/worms) is promoted.¹¹ This micellar growth is general to charged surfactants with added salts as well as to catanionic mixtures. What is evident in our system is that micellar growth is extensive despite the decrease in the hydrophobic volume and in the effective concentration, which oppose the effect of a_0 . This is because NaOA remains in excess, and the effective concentration is still fairly high (it reaches 2.1 wt % at the peak) on this side of the peak, and the micelle is still comprised of mostly long chains. Thus, to the left of the viscosity peak the highly synergistic behavior of the mixture arises mostly from a weakening of the electrostatic interactions that decreases the surface area, thereby driving the micellar growth seen in the cryo-TEM images and the synergistic increase in viscosity.

Micellar Growth in Excess OTAB. Let us now consider the micellar growth as approaching the peak from the right. If we start from pure OTAB, the total concentration is below the CMC, and thus, micelles do not form. However, low levels of the C₁₈ surfactant are sufficient to induce micellization in excess OTAB; therefore, already in the 10/90 NaOA/OTAB sample, mixed spherical micelles dominate the cryo-TEM images. As more NaOA is now added, the effective concentration (measured as the NaOA concentration in the mixture) increases, the hydrophobic volume increases, and the surface area decreases. All three factors act collectively to increase P from $\sim 1/3$ to at least $1/2$ and, thus, to enhance micellization and drive micellar growth. The growth rate, which may be measured by the slopes of curve presented in Figure 1, is lower on this side compared with that characteristic of excess NaOA.

Closer View of the Viscosity Peak and the Effect of Branching. One further aspect that can be explained is why the maximum occurs at 70/30, i.e., shifted toward the NaOA-rich side of Figure 1. As mentioned earlier, the 70/30 weight ratio corresponds to roughly two NaOA molecules for every OTAB; the equimolar scenario corresponds to a weight ratio of 55/45. The reason why the maximum is skewed to the NaOA side is because NaOA is a stronger amphiphile: it has a longer (C₁₈) tail compared to the C₈ tail on OTAB, and accordingly, it has a much lower CMC and a stronger tendency to form micelles. An analogy can be made to the CMC of a mixture of two surfactants,

one cationic and the other anionic. The CMC of the mixture will again be skewed in the direction of the stronger surfactant, i.e., the one with a lower CMC. Indeed, theoretical prediction as well as experimental measurements taken on OTAB/sodium decanosulfonate (C₁₀SO₃Na) showed a minimum at a composition close to equimolar, with a slight shift toward the composition of the pure longer chain.⁴¹ The same trend is seen here (enhanced because of the large difference in tail length between the anionic and cationic surfactants) for the location of the viscosity peak, which from the cryo-TEM images is also the sample with the longest worms.

The above discussion emphasizes the correlation between higher solution viscosities and longer worms (on average). What then is the role of micellar branching? In our cryo-TEM images, we do not see dramatic differences in the extent of branching for the different worm-containing samples. In particular, if we compare 80/20 (left of peak), 70/30 (peak), and 60/40 (right of peak) ratios, there is no clear trend in the density of branch points (white arrows). Note that branch points (junctions) coexist even with spherical micelles and short worms in the 90/10 sample. This is intriguing since spherical micelles and junctions represent limits of high and low curvature, respectively, in micellar solutions.³⁶ However, occasional junctions may arise in multicomponent systems from the inhomogeneous distribution of the surfactants along the micelles. Alternately, junctions may arise spontaneously due to thermodynamic reasons if the energy penalty in forming junctions versus end caps is comparable.³⁶ Regardless of their origin, we find clear evidence of the coexistence of branched and linear micelles in many of our samples. However, for the mixed surfactant system under study, we conclude that branching does not play a significant role in dictating the viscosity maximum.

5. Conclusions

Comprehensive nanostructural analysis conducted via cryo-TEM on the NaOA/OTAB system shows that in the presence of mainly one charged surfactant, cationic or anionic, the solution is populated with small highly curved structures, i.e., spherical micelles. As the oppositely charged surfactant is added because of the other, even in small amounts, a sphere-to-worm micellar transition occurs. The worm micelles grow rapidly and appear to be longer as the mixture composition of the viscosity peak is approached. Analyzing the same data following OTAB addition, we show clearly the decrease in the zero-shear viscosity after the peak is coupled with a decrease in the mean contour length of the worms until the micelles are again spherical.

The key to understanding the assembly in this NaOA/OTAB system is to examine the delicate balance of forces ensuing from the mixing, and their effects on the packing. On one hand, the effective concentration is continuously reduced from 150-fold greater than the CMC in the NaOA-rich side to below the CMC in the pure OTAB system. This is coupled with a continuous decrease in the hydrophobic volume due to the asymmetry of the surfactant chains, which acts to reduce the packing parameter P . On the other hand, the charge density proceeds through a minimum (thus, the area per headgroup and P proceed through a maximum) as the composition is changed from a pure anionic to a pure cationic system. The macroscopic result is a 6-fold increase in the zero-shear viscosity followed by a decrease to the water viscosity when only OTAB is in solution. At the nanometer scale, this is displayed as extensive micellar growth up to the peak, followed by micellar shortening back to the small spherical micelles in the pure OTAB solution.

(41) Shiloach, A.; Blankschtein, D. *Langmuir* **1998**, *14*, 7166–7182.

Junction points exist on both sides of the viscosity peak, as well as in the peak region itself. We suggest that in the NaOA/OTAB system junctions appear as metastable structures and their contribution to the rheology is less pronounced relative to the changes in micelle axial growth. The coexistence of junctions, end caps, and spherical micelles in dilute regions strengthens this assumption.

Also evident from our study is the fact that, in micellar solutions, a pronounced peak in the viscosity as a function of composition may be associated with various growth patterns, and we present micellar shortening as an alternative mechanism to branching in determining the decrease in η_0 after the peak. Our data may be generalized to other mixed systems composed of two micelle-forming surfactants of different charge (either charged and uncharged, or of opposite charge). This conclusion is supported by preliminary data with NaOA/C₁₂TAB that confirm the existence of spherical micelles at a 10/90 ratio (see the Supporting Information). We further suggest that additional viscosity

lowering mechanisms, including branching, will prevail in some other types of mixed surfactant systems and in surfactant/salt systems. Studies of both types of systems are currently in progress.

Acknowledgment. The support of the Israel Science Foundation (Grant 1137/08) and the Russell Berrie Nanotechnology Institute is gratefully acknowledged. The cryo-TEM work was performed at the Cryo-TEM Hannah and George Krumholz Laboratory for Advanced Microscopy at the Technion.

Supporting Information Available: Zero-shear viscosity η_0 of NaOA/C₆TAB and NAOA/OTAB mixtures as a function of C_nTAB weight fraction in the mixture and cryo-TEM image of the 50/50 NaOA/C₆TAB sample which is in the vicinity of the peak (Figure S1) and cryo-TEM image of a 10/90 NaOA/C₁₂TAB mixture (Figure S2). This material is available free of charge via the Internet at <http://pubs.acs.org>.

SUPPORTING INFORMATION

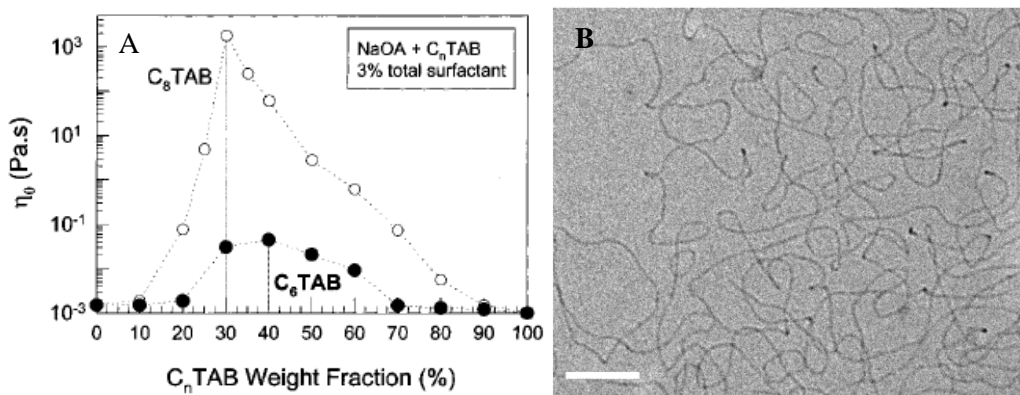


Figure S1. (A) Zero-shear viscosity η_0 of NaOA/C₆TAB and NAOA/OTAB mixtures as a function of C_nTAB weight fraction in the mixture. The total surfactant concentration is 3 wt%. (Figure is reproduced from Raghavan *et al.* 2002.¹). Because C₆TAB by itself does not self-assemble and does not have a CMC it may be considered as a hydrotrope or a strong salt. Thus, it enhanced the viscosity, but only moderately compared with the surfactant OTAB. (B) The cryo-TEM image of the 50/50 NaOA/C₆TAB sample which is in the vicinity of the peak shows that like with OTAB, the high viscosity can be explained by the formation of very long, entangled micelles. Bar = 100 nm.

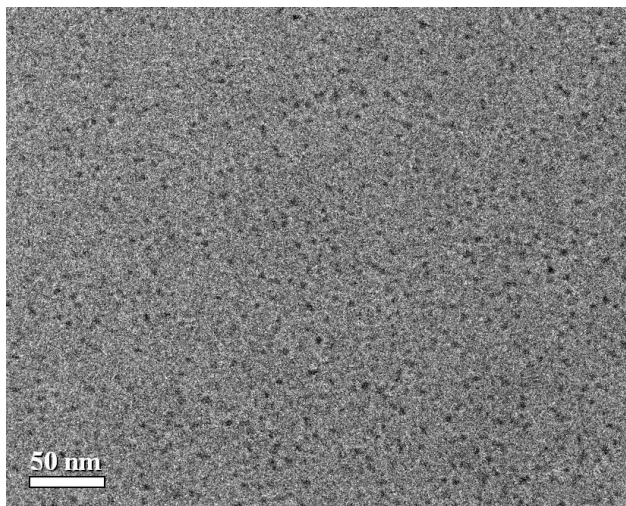


Figure S2. Cryo-TEM image of a 10:90 NaOA/C₁₂TAB mixture. This sample is characterized with a low viscosity of $\sim 10^{-3}$ [Pas·Sec].¹ Like in the NAOA/OTAB system, small spherical micelles dominate in high excess of the C_nTAB surfactant.

Reference

- (1) Raghavan, S. R.; Fritz, G.; Kaler, E. W. *Langmuir* **2002**, *18*, 3797-3803.